

Comment on “Analysis of a Charge-Pump PLL: A New Model” by M. van Paemel

Kuznetsov N.V., Yuldashev M.V., Yuldashev R.V., Blagov M.V.,
Kudryashova E.V., Kuznetsova O.A., Mokaev T.N.

Abstract

In this short communication we comment on the non-linear mathematical model of CP-PLL introduced by V.Paemel. We reveal and obviate some shortcomings in the model.

I. INTRODUCTION

M. van Paemel’s article [1] was the first one where a complete nonlinear mathematical model of CP-PLL is derived. The classical models (see e.g. [2]–[4]) considered approximation of the phase detector dynamics in continuous time and linearization. While approximate models are useful for analysis of small frequency deviations between VCO and Ref signals, Paemel’s models is exact and can also be used for studying out-of-lock behavior.

However, the algorithm suggested in [1] does not always work. Below we reveal and obviate shortcomings in the Paemel’s model and discuss corresponding numerical examples.

N.V. Kuznetsov^{a,b,c}, M.V. Yuldashev^a, R.V. Yuldashev^a, M.V. Blagov^{a,b}, E.V. Kudryashova^a, O.A. Kuznetsova^a, and T.N. Mokaev^a are from (^a) Faculty of Mathematics and Mechanics, Saint-Petersburg State University, Russia; (^b) Dept. of Mathematical Information Technology, University of Jyväskylä, Finland; (^c) Institute of Problems of Mechanical Engineering RAS, Russia; (corresponding author email: nkuznetsov239@gmail.com).

II. NUMERICAL EXAMPLES

The following examples demonstrate that algorithm and formulas suggested by M. van Paemel should be used carefully for simulation even inside allowed area (see original paper Fig 18 and Fig. 22). While the examples are given for the first time, the main idea of Example 1 was already noticed by P. Acco and O. Feely [5], [6]. P. Acco and O. Feely considered only near-locked state, therefore they didn't notice problems with out-of-lock behavior. Example 2 and Example 3 demonstrate problems with out-of-lock behavior, which was not discovered before.

A. Example 1

Consider the following set of parameters and initial state:

$$\begin{aligned} R_2 = 0.2; C = 0.01; K_v = 20; I_p = 0.1; T = 0.125; \\ \tau(0) = 0.0125; v(0) = 1. \end{aligned} \tag{1}$$

Calculation of normalized parameters (equations (27)-(28) and (44)-(45) in [1])

$$\begin{aligned} K_N &= I_p R_2 K_v T = 0.05, \\ \tau_{2N} &= \frac{R_2 C}{T} = 0.016, \\ F_N &= \frac{1}{2\pi} \sqrt{\frac{K_N}{\tau_{2N}}} \approx 0.2813, \\ \zeta &= \frac{\sqrt{K_N \tau_{2N}}}{2} \approx 0.0141, \end{aligned} \tag{2}$$

shows that parameters (1) correspond to allowed area in Fig. 1 (equations (46)–(47), Fig 18 and Fig. 22 in [1]):

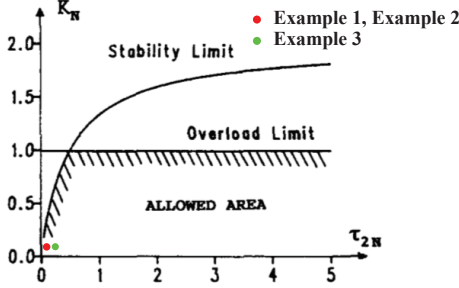


Fig. 18. Stability and overload limits for the PLL normalized loop gain K_N as function of the normalized loop filter time constant τ_{2N} .

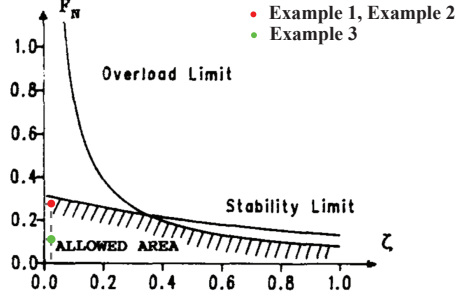


Fig. 22. Stability and overload limits for the PLL normalized natural frequency F_N as a function of the damping factor ζ .

Fig. 1: Parameters for Example 1, Example 2, and Example 3 correspond to allowed area (see Fig 18 and Fig. 22 in [1])

$$F_N < \frac{\sqrt{1+\zeta^2}-\zeta}{\pi} \approx 0.3138, \quad (3)$$

$$F_N < \frac{1}{4\pi\zeta} \approx 5.6438.$$

Now we use the flowchart in Fig. 2 (Fig. 10 in [1]) to compute $\tau(1)$ and $v(1)$: since $\tau(0) > 0$ and $\tau(0) < T$, we proceed to *case 1*) and corresponding relation for $\tau(k+1)$ (equation (7) in [1]):

$$\tau(k+1) = \frac{-I_p R_2 - v(k) + \sqrt{(I_p R_2 + v(k))^2 - \frac{2I_p}{C}(v(k)(T - \tau(k)) - \frac{1}{K_v})}}{\frac{I_p}{C}}. \quad (4)$$

However, the expression under the square root in (4) is negative:

$$(I_p R_2 + v(0))^2 - \frac{2I_p}{C}(v(0)(T - \tau(0)) - \frac{1}{K_v}) = -0.2096 < 0. \quad (5)$$

Therefore the algorithm is terminated with error.

B. Example 2

Consider the same parameters as in Example 1, but $\tau(0) = -0.098$:

$$R_2 = 0.2; C = 0.01; K_v = 20; I_p = 0.1; T = 0.125; \quad (6)$$

$$\tau(0) = -0.098; \quad v(0) = 1.$$

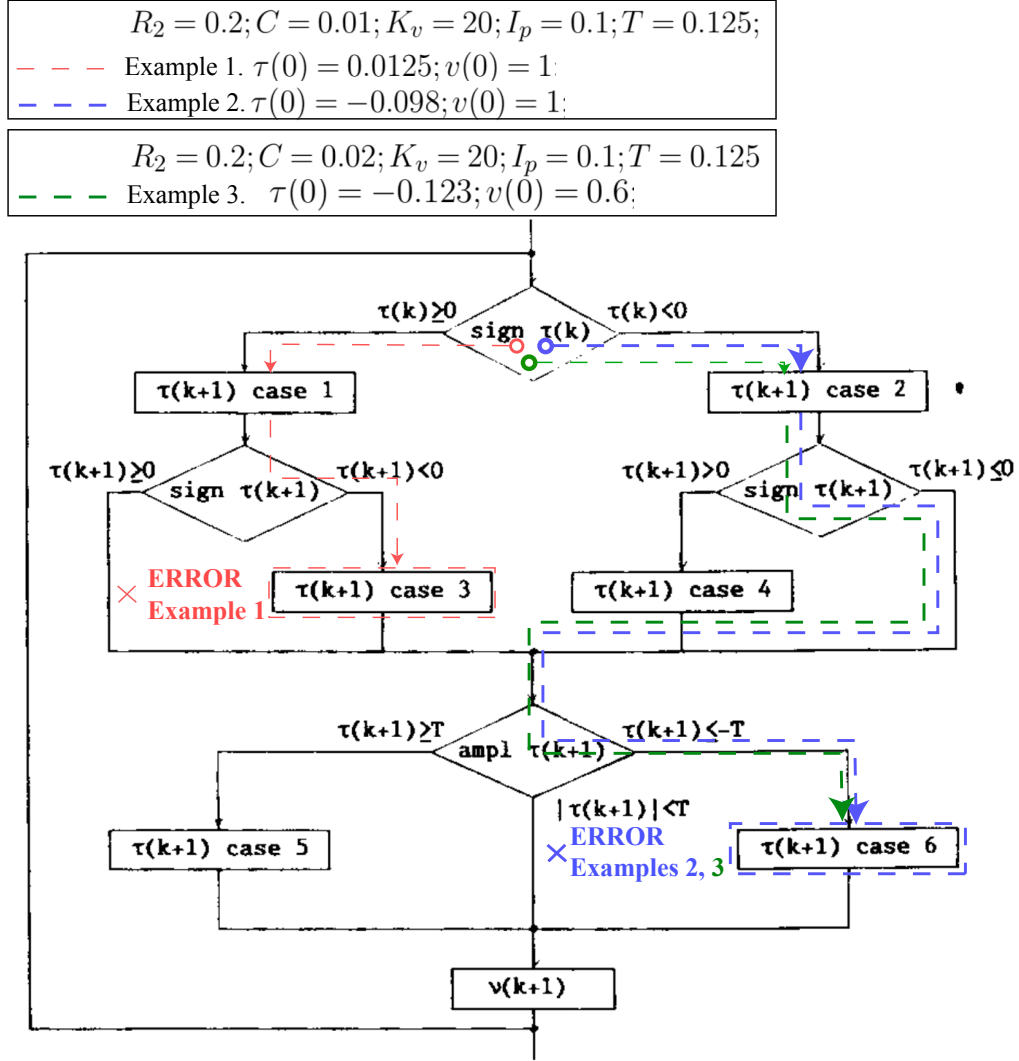


Fig. 10. Flowchart of the algorithm.

Fig. 2: Demonstration of Example 1, Example 2, and Example 3 in the flowchart of the algorithm (see Fig. 10 in [1])

In this case (2), (3), and Fig. 1 are the same as in Example 1, i.e. we are in the “allowed area”. Now we compute $\tau(1)$ and $v(1)$ following the flowchart in Fig. 2: since $\tau(0) < 0$ we

proceed to *case 2*) and corresponding equation of $\tau(k+1)$ (equation (9) in [1]):

$$\begin{aligned}\tau(1) &= \frac{\frac{1}{K_v} - I_p R_2 \tau(0) - \frac{I_p \tau(0)^2}{2C}}{v(0)} - T + \tau(0) = -0.21906, \\ -0.2191 &< -T = -0.125.\end{aligned}\tag{7}$$

This fact indicates cycle-slipping (out of lock). According to the flowchart in Fig. 2 (see Fig. 10 in [1]), we should proceed to *case 6*) and recalculate $\tau(1)$. First step of case 6) is to calculate t_1, t_2, t_3, \dots (equations (16) and (17) in [1]):

$$\begin{aligned}t_n &= \frac{v_{n-1} - I_p R_2 - \sqrt{(v_{n-1} - I_p R_2)^2 - 2 \frac{I_p}{C} \cdot \frac{1}{K_v}}}{\frac{I_p}{C}}, \\ v_n &= v_{n-1} - \frac{I_p}{C} t_n, \\ v_0 &= v(k-1).\end{aligned}\tag{8}$$

Since $k = 0$, then

$$\begin{aligned}t_1 &= \frac{v_0 - I_p R_2 - \sqrt{(v_0 - I_p R_2)^2 - 2 \frac{I_p}{C} \cdot \frac{1}{K_v}}}{\frac{I_p}{C}}, \\ v_1 &= v_0 - \frac{I_p}{C} t_1, \\ v_0 &= v(-1).\end{aligned}\tag{9}$$

However, $v(-1)$ doesn't make sense and algorithm terminates with error.¹ Even if we suppose that it is a typo and $v_0 = v(0)$, then relation under the square root become negative:

$$(v(0) - I_p R_2)^2 - 2 \frac{I_p}{C K_v} = -0.0396 < 0.\tag{10}$$

In both cases the algorithm is terminated with error. Note, that modification of case 2) corresponding to VCO overload (equation (35) in [1]) can not be applied here, since $v(0) > I_p R_2$ (no overload) and $v(1)$ is not computed yet because of the error.

¹However, this can be fixed, by setting $v(-1) = v(0) - \frac{I_p}{C} \tau(0)$.

C. Example 3

Consider parameters:

$$\begin{aligned}\tau(0) &= -0.123; \quad v(0) = 0.6, \\ R_2 &= 0.2; C = 0.02; K_v = 20; I_p = 0.1; T = 0.125.\end{aligned}\tag{11}$$

Similar to (2) and (3)

$$K_N = 0.05, \quad \tau_{2N} = 0.032,\tag{12}$$

$$F_N \approx 0.1989, \quad \zeta = 0.02,$$

$$\begin{aligned}F_N &< \frac{\sqrt{1+\zeta^2}-\zeta}{\pi} \approx 0.3120, \\ F_N &< \frac{1}{4\pi\zeta} \approx 3.9789,\end{aligned}\tag{13}$$

parameters (11) correspond to allowed area in Fig. 1 (equations (46)-(47), Fig. 18 and Fig. 22 in [1]).

Now we compute $\tau(1)$ and $v(1)$ following the flowchart in Fig. 2: since $\tau(0) < 0$ one proceeds to *case 2*) and corresponding equation for computing $\tau(k+1)$ (equation (9) in [1]):

$$\begin{aligned}\tau(1) &= \frac{\frac{1}{K_v} - I_p R_2 \tau(0) - \frac{I_p \tau(0)^2}{2C}}{v(0)} - T + \tau(0) \approx -0.224, \\ -0.224 &< -T = -0.125.\end{aligned}\tag{14}$$

The last inequality indicates cycle-slipping (out of lock). According to the flowchart in Fig. 2 (see Fig. 10 in [1]), one proceeds to *case 6*) and recalculates $\tau(1)$. First step of *case 6*) is to calculate t_1, t_2, t_3, \dots using (8) (see equations (16) and (17) in [1]) until $t_1 + t_2 + \dots + t_n > |\tau(0)|$. Even if we suppose $v(-1) = v(0) - \frac{I_p}{C} \tau(0)$, we get

$$\begin{aligned}t_1 &= 0.0463, \quad v_1 = 1.215; \\ t_2 &= 0.0618, \quad v_2 = 0.983; \\ t_1 + t_2 &= 0.1081 < |\tau(0)| = 0.123.\end{aligned}\tag{15}$$

However, t_3 can not be computed, because the relation under the square root in (8) is negative:

$$(v_2 - I_p R_2)^2 - 2 \frac{I_p}{C} \cdot \frac{1}{K_v} \approx -0.0726. \quad (16)$$

III. CORRECTED DISCRETE TIME MODEL OF CP-PLL

Below we suggest the corrected *discrete time nonlinear mathematical model of CP-PLL*, in which shortcomings are fixed. The problem with flowchart (see Fig. 2) is that the sign of $\tau(k+1)$ computed by *case 1)* is used to decide whether *case 3)* should be used or not. Similarly, *case 2)* always precede *cases 4), 5), 6)* which may lead to errors. However, it is possible to use $\tau(k)$ and $v(k)$ explicitly to select correct formula for $\tau(k+1)$. This allows one to avoid computing square roots of negative numbers, reduce number of cases from 6 to 4, and apply methods from theory of discrete time dynamical systems (see, e.g. [6]).

Here $v(0)$ and $\tau(0)$ are initial conditions (Paemel's notation is used).

$$\tau(k+1) = \begin{cases} \frac{-b + \sqrt{b^2 - 4ac}}{2a}, & \tau(k) \geq 0, \quad c \leq 0, \\ \frac{1}{\omega_{\text{vco}}^{\text{free}} + K_v v(k)} - T + (\tau(k) \bmod T), & \tau(k) \geq 0, \quad c > 0, \\ l_b - T, & \tau(k) < 0, \quad l_b \leq T, \\ \frac{-b + \sqrt{b^2 - 4ad}}{2a}, & \tau(k) < 0, \quad l_b > T, \end{cases} \quad (17)$$

$$v(k+1) = v(k) + \frac{I_p}{C} \tau(k+1).$$

$$\begin{aligned}
a &= \frac{K_v I_p}{2C}, \\
b &= b(v(k)) = \omega_{\text{vco}}^{\text{free}} + K_v v(k) + K_v I_p R_2, \\
c &= c(\tau(k), v(k)) = (T - (\tau(k) \bmod T)) (\omega_{\text{vco}}^{\text{free}} + K_v v(k)) - 1, \\
l_b &= l_b(\tau(k), v(k)) = \frac{1 - S_{l_a}}{K_v v(k) + \omega_{\text{vco}}^{\text{free}}}, \\
S_{l_a} &= S_{l_a}(\tau(k), v(k)) = S_{l_k} \bmod 1, \\
S_{l_k} &= S_{l_k}(\tau(k), v(k)) = - \left(K_v v(k) - I_p R_2 K_v + \omega_{\text{vco}}^{\text{free}} \right) \tau(k) + K_v I_p \frac{\tau(k)^2}{2C}, \\
d &= d(v(k)) = S_{l_a} + T(K_v v(k) + \omega_{\text{vco}}^{\text{free}}) - 1.
\end{aligned}$$

Here VCO frequency is $f_{\text{vco}} = \omega_{\text{vco}}^{\text{free}} + K_v v_c$, and $\omega_{\text{vco}}^{\text{free}}$ is a free-running (quiescent) frequency (in V.Paemel's paper $\omega_{\text{vco}}^{\text{free}} = 0$). If at some point VCO becomes overloaded one should stop simulation or use another set of equations, based on ideas similar to (34) and (35) in [1].

Overload conditions are

$$\begin{aligned}
\tau(k) > 0 \text{ and } v(k) + \frac{\omega_{\text{vco}}^{\text{free}}}{K_{\text{vco}}} - \frac{I_p}{C} \tau_k &< 0, \\
\tau(k) < 0 \text{ and } v(k) + \frac{\omega_{\text{vco}}^{\text{free}}}{K_{\text{vco}}} - I_p R_2 &< 0.
\end{aligned} \tag{18}$$

Remark that following the ideas from [1], [5], [7], the number of parameters in (17) can be reduced to just two (α and β) by the following change of variables

$$\begin{aligned}
s(k) &= \frac{\tau(k)}{T}, \quad \omega(k) = T (\omega_{\text{vco}}^{\text{free}} + K_v v(k)) - 1, \\
\alpha &= K_v I_p T R_2, \quad \beta = \frac{K_v I_p T^2}{2C}.
\end{aligned} \tag{19}$$

IV. NUMERICAL EXAMPLES FOR CORRECTED MODEL

Consider application of the corrected model (17) to numerical examples from section II. All three examples assume $\omega_{\text{vco}}^{\text{free}} = 0$.

A. Example 1

By (17) and (1) we calculate value of c :

$$c = (T - (\tau(0) \bmod T))K_v v(0) - 1 = 1.2500 \quad (20)$$

and since $\tau(0) \geq 0$ and $c > 0$ we get

$$\begin{aligned} \tau(1) &= \frac{1}{K_v v(0)} - T + (\tau(0) \bmod T) = -0.0625, \\ v(1) &= v(0) + \frac{I_p}{C} \tau(1) = 0.3750. \end{aligned} \quad (21)$$

Illustration of this example is shown in Fig. 3.

Note, that in this case there is no VCO overload (no saturation), since the filter output (VCO input) is positive, see Fig. 3.

B. Example 2

By (17) and (6) we have $l_b \approx 0.0059$. Since $l_b \leq T$, then $\tau(1) \approx -0.1191, v(1) \approx -0.1906$. In this case the VCO is overloaded (see Fig. 4). Model (17) correctly detects overload by (18)

$$v(1) + \frac{\omega_{\text{vco}}^{\text{free}}}{K_{\text{vco}}} - I_p R_2 \approx -0.2106 < 0 \quad (22)$$

and stops simulation.

C. Example 3

Note, that in this case VCO is not overloaded, since the filter output (VCO input) is positive, see Fig. 5. Equations (17) allow to correctly calculate next step:

$$\tau(1) = 0, \quad v(1) = 10. \quad (23)$$

V. COMPARISON OF SIMULINK VS V.PAEMEL'S MODEL VS CORRECTED MODEL

Correctness of proposed model was verified by extensive simulation in Matlab Simulink. Circuit level model in Matlab Simulink was compared with original model by V. Paemel and proposed model (see parameters (24) and Fig. 6).

$$\begin{aligned}\tau(0) &= 0; \quad v(0) = 10, \\ R_2 &= 1000; C = 10^{-6}; K_v = 500; I_p = 10^{-3}; T = 10^{-3}. \\ \tau_{2N} &= 1; K_N = 0.5; F_N = 0.1125; \zeta = 0.3536.\end{aligned}\tag{24}$$

Based on simulation for this set of parameters all three models produce almost the same results.

VI. CONCLUSIONS

There were many attempts to generalize equations derived in [1] for higher-order loops (see, e.g. [8]–[13]), but the resulting transcendental equations can not be solved analytically without using approximations.

ACKNOWLEDGMENTS

The work is supported by the Russian Science Foundation project 19-41-02002.

REFERENCES

- [1] M. van Paemel, “Analysis of a charge-pump PLL: A new model,” *IEEE Transactions on communications*, vol. 42, no. 7, pp. 2490–2498, 1994.
- [2] F. Gardner, *Phaselock techniques*. John Wiley & Sons, 2005.
- [3] R. Best, *Phase-Locked Loops: Design, Simulation and Application*, 6th ed. McGraw-Hill, 2007.
- [4] G. Leonov, N. Kuznetsov, M. Yuldashev, and R. Yuldashev, “Hold-in, pull-in, and lock-in ranges of PLL circuits: rigorous mathematical definitions and limitations of classical theory,” *IEEE Transactions on Circuits and Systems–I: Regular Papers*, vol. 62, no. 10, pp. 2454–2464, 2015.
- [5] P. Acco, “Study of the loop ‘a phase lock: Hybrid aspects taken into account,” Ph.D. dissertation, Toulouse, INSA, 2003.
- [6] O. Feely, P. F. Curran, and C. Bi, “Dynamics of charge-pump phase-locked loops,” *International Journal of Circuit Theory and Applications*, 2012.
- [7] P. Curran, C. Bi, and O. Feely, “Dynamics of charge-pump phase-locked loops,” *International Journal of Circuit Theory and Applications*, vol. 41, no. 11, pp. 1109–1135, 2013.

- [8] P. K. Hanumolu, M. Brownlee, K. Mayaram, and U.-K. Moon, “Analysis of charge-pump phase-locked loops,” *IEEE Transactions on Circuits and Systems I: Regular Papers*, vol. 51, no. 9, pp. 1665–1674, 2004.
- [9] B. Shakhtarin, A. Timofeev, and V. Sizykh, “Mathematical model of the phase-locked loop with a current detector,” *Journal of Communications Technology and Electronics*, vol. 59, no. 10, pp. 1061–1068, 2014.
- [10] C. Bi, P. F. Curran, and O. Feely, “Linearized discrete-time model of higher order charge-pump pll’s,” in *Circuit Theory and Design (ECCTD), 2011 20th European Conference on*. IEEE, 2011, pp. 457–460.
- [11] C. Hangmann, C. Hedayat, and U. Hilleringmann, “Stability analysis of a charge pump phase-locked loop using autonomous difference equations,” *IEEE Transactions on Circuits and Systems I: Regular Papers*, vol. 61, no. 9, pp. 2569–2577, 2014.
- [12] S. Milicevic and L. MacEachern, “Time evolution of the voltage-controlled signal in charge pump pll applications,” in *Microelectronics, 2008. ICM 2008. International Conference on*. IEEE, 2008, pp. 413–416.
- [13] S. Sancho, A. Suárez, and J. Chuan, “General envelope-transient formulation of phase-locked loops using three time scales,” *IEEE Transactions on Microwave Theory and Techniques*, vol. 52, no. 4, pp. 1310–1320, 2004.

ILLUSTRATIONS FOR NUMERICAL EXAMPLES

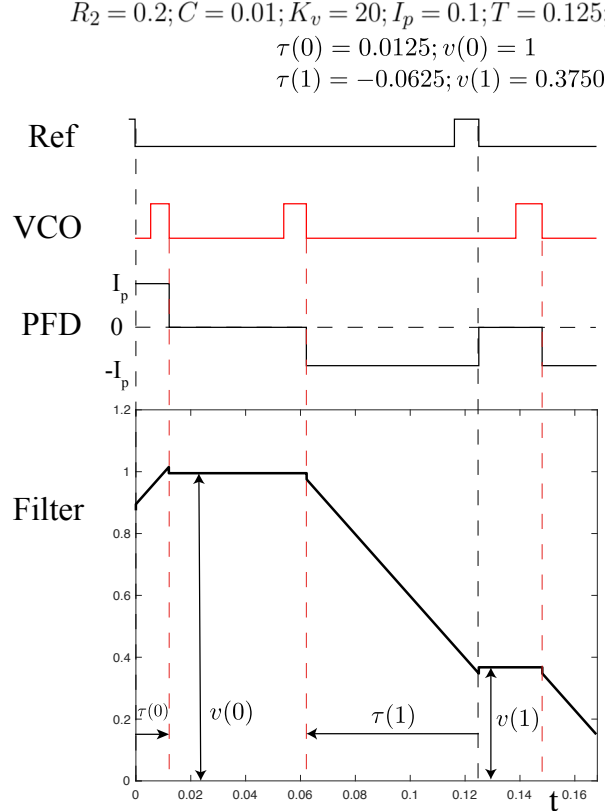


Fig. 3: Application of corrected model to Example 1: Reference signal, VCO output, PFD output, and filter output.

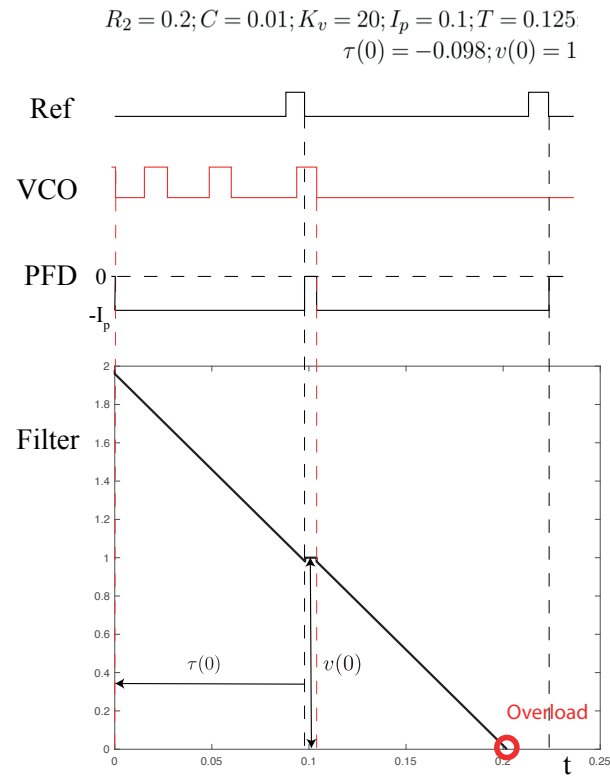


Fig. 4: Application of corrected model to Example 2: Reference signal, VCO output, PFD output, and filter output.

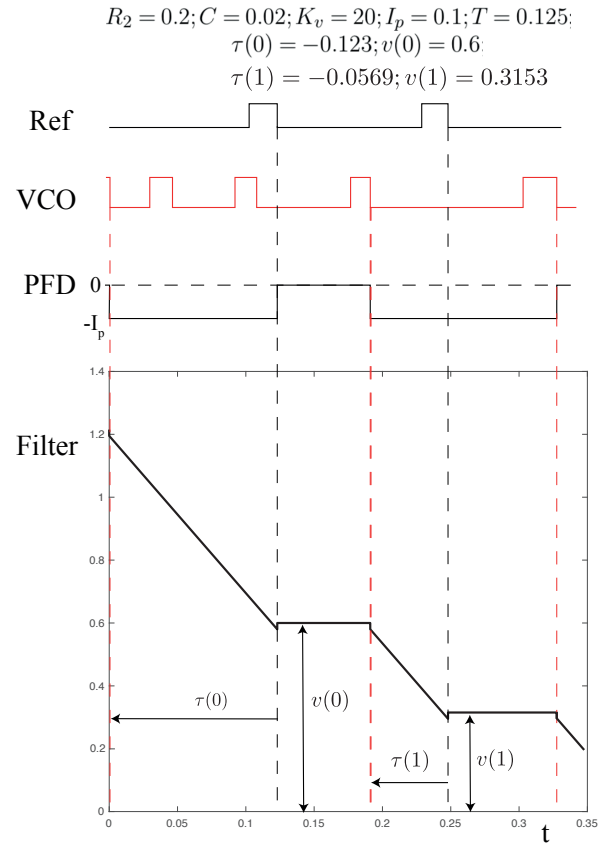


Fig. 5: Application of corrected model to Example 3: Reference signal, VCO output, PFD output, and filter output.

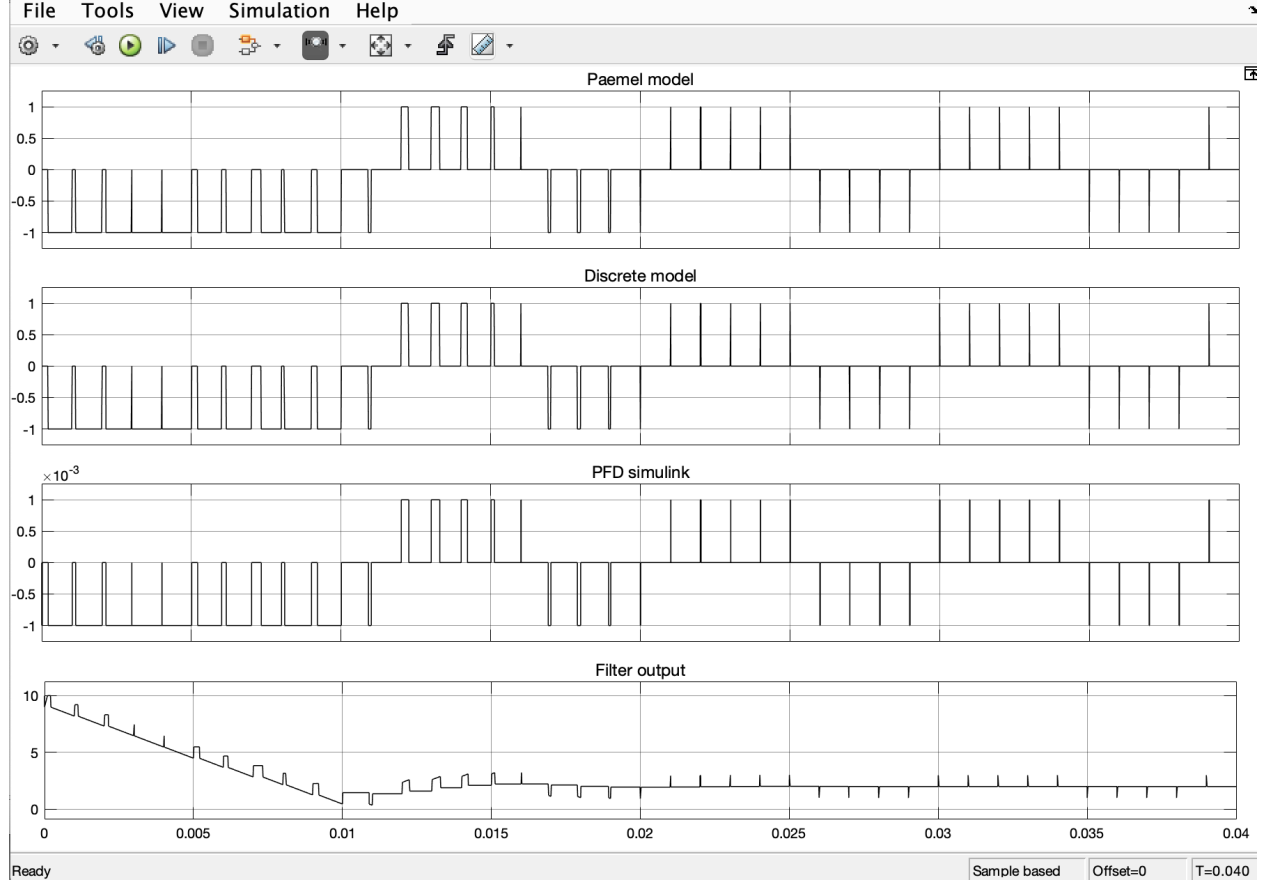


Fig. 6: Comparison of PFD outputs of Simulink model (PFD Simulink) vs V.Paemel's model (Paemel model) vs Corrected model (Discrete model). Lower subfigure demonstrates output of Loop filter. For considered set of parameters ($\tau(0) = 0; v(0) = 10; R_2 = 1000; C = 10^{-6}; K_v = 500; I_p = 10^{-3}; T = 10^{-3}; \tau_{2N} = 1; K_N = 0.5; F_N = 0.1125; \zeta = 0.3536$) all three models produce almost the same results.